

Retinal Fundus Multi-Disease Image Dataset (RFMiD) 2.0: A Dataset of Frequently and Rarely Identified Diseases

Sachin Panchal ^{1,*}, Ankita Naik ¹, Manesh Kokare ^{1,*}, Samiksha Pachade ², Rushikesh Naigaonkar ³, Prerana Phadnis ⁴ and Archana Bhanghe ⁵

- ¹ Center of Excellence in Signal and Image Processing, Shri Guru Gobind Singhji Institute of Engineering and Technology, Nanded 431606, Maharashtra, India
² School of Biomedical Informatics, The University of Texas Health Science Center, 7000 Fannin St Suite 600, Houston, TX 77030, USA
³ Shri Ganapati Netralaya State of Art Eye Care Hospital, Jalna 431203, Maharashtra, India
⁴ Lions Eye Hospital, Nanded 431603, Maharashtra, India
⁵ Keya Eye Clinic, Pune 411062, Maharashtra, India
* Correspondence: 2021pec202@snggs.ac.in (S.P.); mbkokare@snggs.ac.in (M.K.); Tel.: +91-9665602266 (S.P.)

Abstract: Irreversible vision loss is a worldwide threat. Developing a computer-aided diagnosis system to detect retinal fundus diseases is extremely useful and serviceable to ophthalmologists. Early detection, diagnosis, and correct treatment could save the eye's vision. Nevertheless, an eye may be afflicted with several diseases if proper care is not taken. A single retinal fundus image might be linked to one or more diseases. Age-related macular degeneration, cataracts, diabetic retinopathy, Glaucoma, and uncorrected refractive errors are the leading causes of visual impairment. Our research team at the center of excellence lab has generated a new dataset called the Retinal Fundus Multi-Disease Image Dataset 2.0 (RFMiD2.0). This dataset includes around 860 retinal fundus images, annotated by three eye specialists, and is a multiclass, multilabel dataset. We gathered images from a research facility in Jalna and Nanded, where patients across Maharashtra come for preventative and therapeutic eye care. Our dataset would be the second publicly available dataset consisting of the most frequent diseases, along with some rarely identified diseases. This dataset is auxiliary to the previously published RFMiD dataset. This dataset would be significant for the research and development of artificial intelligence in ophthalmology.

Dataset: <https://zenodo.org/record/7505822>.

Dataset License: CC BY 4.0

Keywords: data analysis; ocular diseases; retinal fundus image dataset; data annotation; multilabel classification



Citation: Panchal, S.; Naik, A.; Kokare, M.; Pachade, S.; Naigaonkar, R.; Phadnis, P.; Bhanghe, A. Retinal Fundus Multi-Disease Image Dataset (RFMiD) 2.0: A Dataset of Frequently and Rarely Identified Diseases. *Data* **2023**, *8*, 29. <https://doi.org/10.3390/data8020029>

Academic Editor: Sameer Antani

Received: 31 December 2022

Revised: 19 January 2023

Accepted: 25 January 2023

Published: 28 January 2023



Copyright: © 2023 by the authors. Licensee MDPI, Basel, Switzerland. This article is an open access article distributed under the terms and conditions of the Creative Commons Attribution (CC BY) license (<https://creativecommons.org/licenses/by/4.0/>).

1. Summary

Multiple retinal diseases are responsible for partial or complete vision impairment. Numerous equally significant causes of vision impairment must be addressed, including age-related macular degeneration and Glaucoma. In addition, chronic illnesses such as diabetes can lead to ocular damage, infectious eye disease, and diabetic retinopathy. However, vision loss can impair people of all ages. Most people who are blind or have vision problems are over 50 [1]. A Disease can be identified when lesions or other abnormalities are seen in the retinal fundus image. However, early disease detection can save a subject's vision. Therefore, a complete pathological test should be conducted once a year [2].

A typical retinal fundus image comprises the retina's background, blood vessels, macula, and fovea. In a fundus image, various diseases can be seen in specific areas of the retina. Cotton-wool spots on the retina are typical ocular symptoms of several medical

conditions, including diabetes mellitus, systemic hypertension, leukemia, AIDS, etc [3,4]. Some diseases may affect the standard structure optic disc and the cup. A medical test cannot provide much information on the detection of Glaucoma because it is a multifocal disease. Few structural changes in the area of the retinal layers and optic nerve are caused by the progression of Glaucoma. Numerous structural changes are performed for glaucoma identification, such as the Cup-to-Disc Ratio (CDR) and Rim-to-Disc Ratio (RDR) [5]. Glaucoma can permanently damage the optic nerves and result in blindness if untreated. Often, relatively mild or no symptoms accompany this progressive and irreversible damage to the optic nerves [6].

An image may illustrate one or more symptoms of several diseases. The primary challenge with Multilabel Dataset (MLD) is the imbalanced form, where the samples and their corresponding labels are not evenly distributed throughout the data space. When handling the imbalance challenge in an MLD, the problem transformation and adaptation methodologies used for the MLD task are inadequate. A generally imbalanced dataset presents a significant problem in various real-world applications, including biomedical engineering [7–10]. The RFMiD2.0 Dataset is auxiliary to our previously published Retinal Fundus Multi-Disease Image Dataset (RFMiD). RFMiD2.0 is a collection of 49 rare and frequently observed diseases. Optic Neuritis, Retinal Detachment, Retinal Holes and Tear, Silicone Oil-filled Eye, and Hypertension are some diseases that are identified by ophthalmologists and included in the dataset. The overall process of generating a database is illustrated in Figure 1.

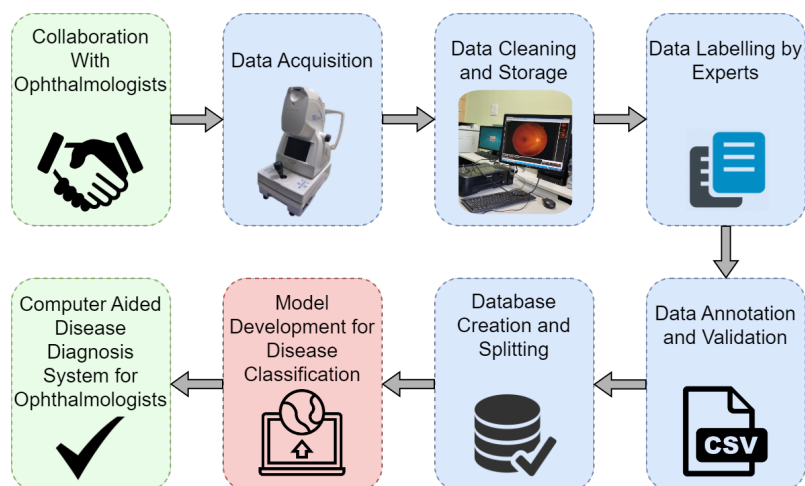


Figure 1. Process of creating dataset by taking consent from ophthalmologists to develop Computer Aided Disease Diagnosis (CADD) System.

Researchers could get in touch with the ophthalmologist to carry out the collaborative work needed to compile data for the dataset. Three eye specialists will collect the retinal fundus images from the subject. The researchers receive the stored data. Then the information that was gathered would be cleaned by removing faulty images, which will be labeled and annotated by the doctors. Eye professionals have a responsibility to provide accurate information. After cross-verifying the labeled images, the final dataset would be divided into training, validation, and testing sets. This dataset would significantly help researchers worldwide to design a disease classification model. The computer-aided disease diagnosis (CADD) system can be developed utilizing artificial intelligence or traditional methods and techniques. However, artificial intelligence (AI) is a new technology in the area of medical imaging. Compared to the conventional imaging methodology, which primarily relies on human effort, AI enables the development of imaging solutions that are more secure, accurate, and productive. However, the most current and reliable uses of AI in clinical research are evaluation and diagnosis [11]. Modern deep learning algorithms

have recently developed an automated and dependable medical image classification with superior accuracy, on par with that obtained by professionals [7].

The specifications of the dataset are represented in Table 1.

Table 1. Specifications of dataset.

Subject area	Ophthalmology, Biomedical Data
More specific subject area	Multiple Disease Classification of Retinal fundus images
Type of data	Images, CSV files
How data was acquired	TOPCON TRC-NW300
Data format	Labelling and Annotation of .JPEG, .PNG image files into .CSV files
Experimental factors	Most of the patients were subjected to mydriasis with one drop of tropicamide at 0.5% Concentration. The non-Mydriatic process is conducted for some subjects.
Experimental features	The fundus images were captured with position and orientation of the patient sitting upright with 40.7 mm (TOPCON TRC-NW300) and 42 mm (CARL ZEISS FF450) working distance between lenses and examined eye using non-invasive fundus camera.
Data source location	State of Art Eye Care Hospital, Shri Ganpati Netralaya located at Jalna, Maharashtra, India. Center of Excellence in Signal and Image Processing, SGGGS Institute of Engineering and Technology, Nanded, Maharashtra, India.

2. Data Description

The RFMiD2.0 is an 860-image dataset that includes images from multiple retinal diseases. Experts assigned labels and annotations to each image. The RFMiD2.0 dataset was further divided into the two categories mentioned below.

- Firstly, retinal fundus images were screened into healthy and disease-risk categories.
- Further, the disease-risk category was classified into 49 different sub-classes.

The RFMiD2.0 dataset is a Multilabel Multiclass Imbalanced Dataset (MMID), consisting of 860 images of 49 frequently and rarely observed diseases, within normal-range images. The entire dataset was split into approximately three sets—a training set, a validation set, and a testing set—in a ratio of 60:20:20. This dataset includes images in PNG and .JPEG format. The labels are available in CSV format. RFMiD_2_Training_labels.CSV, RFMiD_2_Validation_labels.CSV, RFMiD_2_Testing_labels.CSV includes training, validation, and testing set labels, respectively.

3. Experimental Design, Materials, and Methods

3.1. Ethics Statement

The participants in this study gave informed consent. According to the local ethics committee rules, clinical practice standards, and medical research standards, appropriate precautions were taken to preserve subjects' privacy. The Shri Guru Gobind Singhji Institute of Engineering and Technology, Nanded (MS), India, Local Research Ethical Approval Committee approved the dataset.

3.2. Data Acquisition

Two cameras, the TOPCON TRC-NW300 from TOPCON CORPORATION, Tokyo, Japan and CARL ZEISS FF450 from Carl Zeiss Meditec AG, Jena, Germany were used for image acquisition. CARL ZEISS FF450 was utilized for acquiring images from subjects who visited Shri Ganpati Netralaya Jalna for diagnosis and treatment. In contrast, TOPCON TRC-NW300 was available in the state-of-the-art center of excellence in signal and image

processing lab at our institute in Nanded. The imaging technology in cameras enables a non-invasive, painless means of screening the retina. Furthermore, retinal imaging technology makes it convenient to use and capable of detecting conditions that cause retinopathy. However, the operator's skills are equally important in capturing high-resolution images with hidden features [2].

3.2.1. Preparation before Taking Samples

Mydriasis is dilating the pupils, and was carried out using one drop of tropicamide at a 0.5% concentration. The subjects were asked to sit upright while capturing a fundus image.

3.2.2. Quality of Image

The 860 images used for this dataset were selected from the collected images. IMAGENet-i-base system of TOPCON was used for image processing and to maintain quality with TRC-NW300 retinal camera.

3.2.3. Camera Specifications

TOPCON TRC-NW300 [12]

- Eight-megapixel, high-quality images were produced by the integrated digital CCD camera. The angle of view was 45°.
- Fundus camera type: non-Mydriatic
- Auto-focus, auto-exposure, and auto-shoot are vital camera features.

CARL ZEISS FF450 [13]

- FF 450plus Fundus Camera and VISUPAC Digital Imaging System are seamlessly integrated for exceptional image quality, operation, and diagnostic adaptability.
- Through reciprocal calibration, the VISUPAC system and the FF 450plus Fundus Camera continuously deliver a distinct level of precision.
- For the fine detail of the macula and optic nerve, the Zeiss FF450 plus Fundus Camera offers three field angles: 50°, 30°, and the smaller 20° field.

3.3. Annotation of Images

At first, two ophthalmologists independently classified each image. Some fundus images included one or more labels. Multiple labels were applied to a single image if fundus imaging revealed the presence of more than one disease. When there were discrepancies in the diagnostic evaluations after the ophthalmologists had finished initially labeling the fundus images, the labels were verified and confirmed. The labels offered by the specialists are further explained.

Within Normal Limit (WNL): Normal retinal anatomical structure consists of two fundamental parts that can be segmented using various algorithms. Optic discs and blood vessels can be detected and differentiated for retinal image analysis [14]. The retina is clear in normal fundus images, and the retinal arteriolar lumen and venules run through the retinal layer, making them the primary elements of the retina. These are easily visible [15].

Asteroid Hyalosis (AH): AH is the typical ophthalmologist finding. Asteroid hyalinitis (AH) is observed as yellow–white dazzling, reflecting particles enclosed by densely adhered fibrils [16]. It is necessary to conduct an accurate ocular evaluation to diagnose this illness as shown in Figure 2a.

Anterior Ischemic Optic Neuropathy (AION): The optic nerve's swollen and pale presence is observed on the retina. Moreover, there are retinal cotton wool spots at the anterior pole, and this artery can cause temporary central retinal artery occlusion. Ischemic optic neuropathies (IONs) are the most frequent acute optic neuropathy in patients older than 50. The signs of AION are reduced clarity of vision, color blindness, and other visual defects [17,18]. Figure 2b shows an image of AION.

Age-Related Macular Degeneration (ARMD): ARMD is one of the leading causes of significant vision loss, including vision impairment, among the population, usually occurring in those over 60. Lipoprotein deposits and acellular wastes are responsible for drusen.

Retinal pigment epithelium abnormalities, drusen, and choroidal neovascular membrane formation are referred to as ARMD. The presence of visible spots of degeneration in the retinal fundus images is used to identify the ARMD as shown in Figure 2c [19–21]. Furthermore, geographic atrophy and drusen that extend to the macula center are indications of advanced non-neovascular age-related macular degeneration [22].

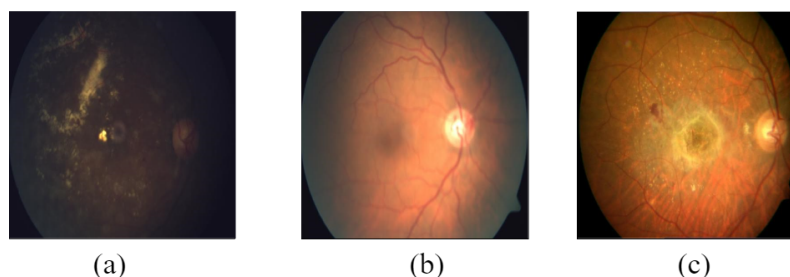


Figure 2. Images of (a) Asteroid Hyalosis (AH), (b) Anterior ischemic optic neuropathy (AION), and (c) Age-Related Macular Degeneration (ARMD).

Branch Retinal Vein Occlusion (BRVO): One of the most frequent forms of acquired microvascular abnormalities in retinal fundus images, and a common cause of vision loss, is retinal vein occlusion. The presence of retinal edema, surface-deep retinal hemorrhages, intraretinal abnormalities, anastomotic vessels, and venous dilation in the region of the retina corresponding to the occluded vein were all considered symptoms of branch retinal vein occlusion [23].

Coloboma (CB): Coloboma impacts the morphological structure and functionality of the eye. Coloboma in the macula and optic disc may threaten the subject's vision, increasing the risk of retinal degeneration [24].

Choroidal folds (CF): Undulations of the choroid, Bruch's membrane, retinal pigment epithelium, and neurosensory retina are called chorioretinal folds. CFs are a clinical symptom that must be looked at if they are assumed to be related to various extraocular and ocular illnesses. Recent developments have improved the characterization of CFs in retinal imaging. The development of choroidal neovascularization is just one of the visual complications that can result from chronic CFs that may be picked up by retinal imaging [25].

Images of BRVO, CB, and CF are shown in Figure 3a–c, respectively.

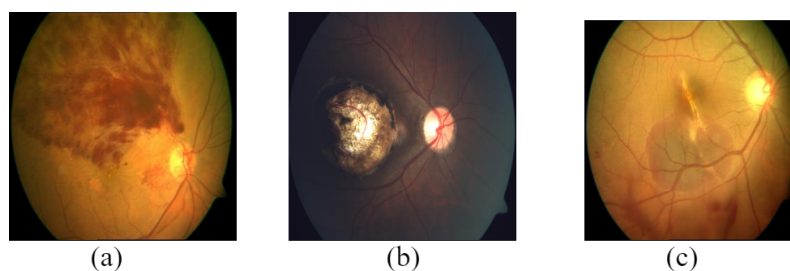


Figure 3. Images of (a) Branch Retinal Vein Occlusion (BRVO), (b) Coloboma (CB), and (c) Choroidal Folds (CF).

Collateral (CL): These are vessels that grow inside the framework of the retinal vascular network that is already in place. In other words, veins are connected to veins, and arteries are connected to arteries. Collaterals emerge from the retinal capillary bed, joining nearby capillaries that are blocked or unblocked or spread around obstructions in a single vessel. Atherosclerosis occurs when veins and, less frequently, arteries are connected. These canals often have slow, infrequently normal flow [26].

Macular Edema (ME): ME is a common pathologic sequela of the retina that can result from several pathological diseases, including diabetic retinopathy, central or branch retinal

vein blockage, intraocular inflammation, and, most frequently, cataract surgery. According to histological investigations, the macula region often exhibits radially oriented cystoid pockets filled with ophthalmoscopically clear fluid. These cysts resemble regions of the retina where the cells appear to have been dispersed [27].

Neovascularization (NV): Proliferative Diabetic Retinopathy (PDR) can result in the microvascular blockage of retinal blood vessels. Moreover, the retina responds by growing new, tiny blood vessels, known as neovascularization. If these fragile new blood vessels break, there may be vitreous hemorrhage. Neovascularization in the retina and the optic disc is a characteristic of PDR [28]. The relevant images of CL, ME, and NV are presented in Figure 4a–c.

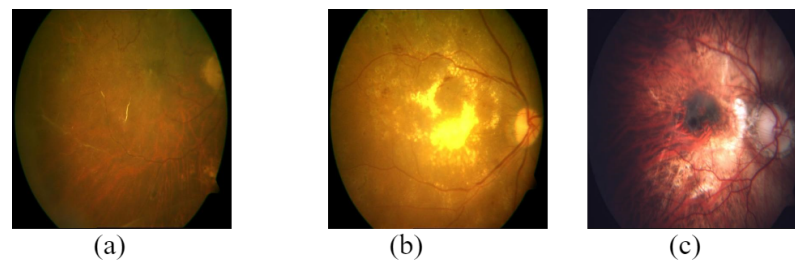


Figure 4. Images of (a) Collateral (CL), (b) Macular Edema (ME), and (c) Neovascularization (NV).

Central Retinal Artery Occlusion (CRAO): CRAO is characterized by retinal infarction, cherry red spots, and retinal arterial irregularities, as well as the absence of residual retinal circulation or poor residual retinal circulation on fluorescein fundus as shown in Figure 5a. Due to the sudden, profound sight loss, this is an ocular emergency. There is a vast body of literature on its numerous topics, which is rife with severe debates and myths, especially regarding its management [29].

Chorioretinitis (CRS): Uveitis of the choroid and retina of the eye are both inflamed in chorioretinitis, a kind of uveitis that affects the posterior region of the eye. The vascular layer of the eye, or choroid, is located between the retina and the sclera. The choroid is in control of providing the outer layers of the retina with a circulatory supply. Therefore, inflammation of these layers might result in issues that could endanger vision [30]. Figure 5b presents CRS image.

Central retinal vein occlusion (CRVO): The presence of retinal edema, optic disc edema, sporadic shallow, and deep retinal hemorrhages, and venous dilatation were considered to be signs of central retinal vein occlusion as shown in Figure 5c. Hypertension, retinal microvascular abnormalities, renal impairment, and hypertriglyceridemia are linked with retinal vein occlusion [31].

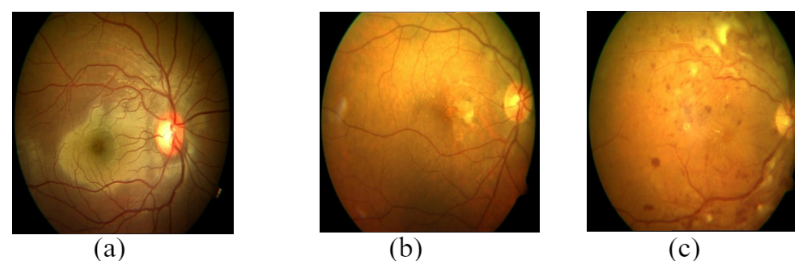


Figure 5. Images of (a) Central Retinal Artery Occlusion (CRAO), (b) Chorioretinitis (CRS), and (c) Central retinal vein occlusion (CRVO).

Cysticercosis (CSC): A preventable endemic cause of blindness in India is cysticercosis. This is a parasitic infestation brought on by *Cysticercus cellulose*, which is *Taenia sodium*'s larval stage [32].

Cotton Wool Spots (CWS): Microinfarction-related white patches on the retinal surface (shown in Figure 6b) are called cotton wool spots. Several conditions, such as viral

infection, diabetes, hypertension and high coagulation conditions, cause CWS [33,34]. Figure 6b,c, respectively, depict images of CWS and CSC.

Drusens (DN): Drusens are fatty formations that appear in retinal fundus imaging as yellowish or whitish, blurry, bright spots as shown in Figure 7a. The visible boundaries, size, and shape of the drusens are judging parameters when grading the macular degeneration disease. The drusens are further classified as soft and hard drusens. Compared to soft drusens, which have hazy boundaries, hard drusens are smaller and more clearly defined [35].

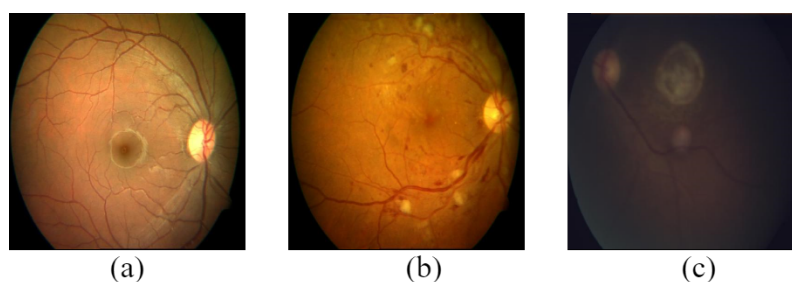


Figure 6. Images of (a) Central Serous Retinopathy (CSR), (b) Cotton Wool Spots (CWS), and (c) Cysticercosis (CSC).

Diabetic Retinopathy (DR): Diabetic retinopathy (DR) is constituted by microvascular damage to the retinal structure in hyperglycemia [36]. DR is characterized by one or more vascular changes such as microaneurysms, exudates, hemorrhages, cotton wool spots, neovascularization, and other microvascular abnormalities. Furthermore, it is classified into non-proliferative and proliferative DR categories [37,38].

Exudation (EX): The progress in diabetic retinopathy disease leads to a blockage in the retinal blood vessels, which is responsible for the formation of microscopic abnormalities. These abnormalities are referred to as exudates shown in Figure 7b. Furthermore, exudates are classified into soft and hard exudates. Soft exudates appear as pale yellow or white patches with unclear boundaries, whereas hard exudates are yellow patches in the retina [38].

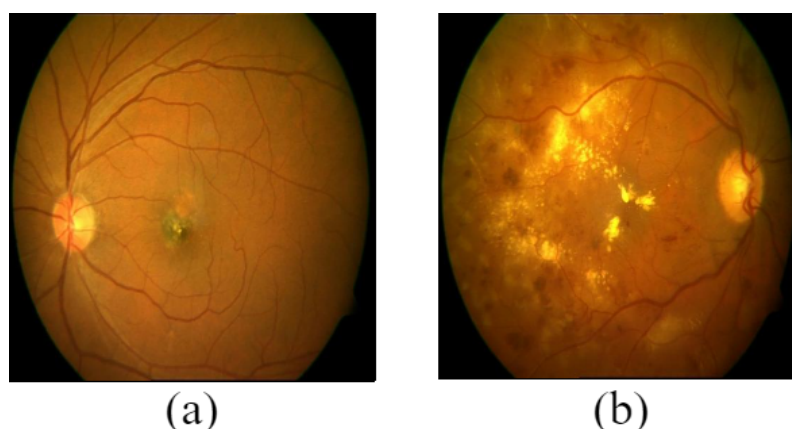


Figure 7. Images of (a) Drusens (DN), (b) Exudation (EX).

Epiretinal Membrane (ERM): ERM is avascular (having few or no blood vessels), semitranslucent, fibrocellular membranes that grow on the retina's inner surface. They are also referred to as cellophane maculopathy or macular puckers. They often have few symptoms and can be easily detected, but can occasionally can induce painless vision loss and metamorphopsia (visual distortion). In general, ERMs are most symptomatic when they damage the macula, the central region of the retina that aids in the ability to detect fine detail used to read and recognize faces [39]. Figure 8a represents an image of ERM.

Giant Retinal Tear (GRT): Giant retinal tears are characterized as circumferential full-thickness tears of the retina that extend beyond 90 degrees and are linked to vitreous detachment (Figure 8b). Due to the numerous issues and technical problems involved, managing them presents enormous tasks. Although GRTs can happen independently, they are frequently linked to several diseases, such as ocular trauma, extreme myopia, aphakia, pseudophakia, collagen-related genetic abnormalities, and young age [40].

Hemorrhagic Pigment Epithelial Detachment (HPED): Separation between the RPE and the innermost part of Bruch's membrane is a characteristic of retinal pigment epithelial detachments (PEDs) shown in Figure 8c. The blood patch, serous exudate, drusenoid material, fibrovascular tissue, or a mix of the above can fill the gap left by this separation [41].

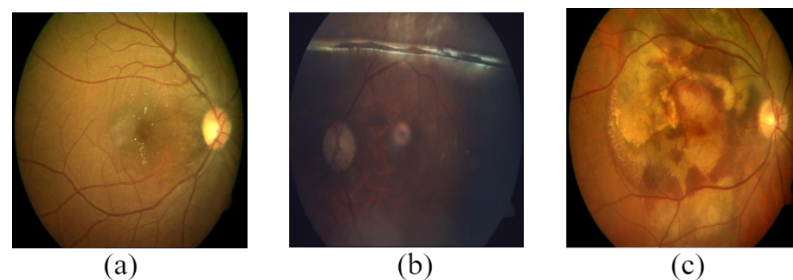


Figure 8. Images of (a) Epiretinal Membrane (ERM), (b) Giant Retinal Tear (GRT), and (c) Hemorrhagic Pigment Epithelial Detachment (HPED).

Idiopathic Intracranial Hypertension (IIH): Increased intracranial pressure is the hallmark of the complicated neuro-ophthalmological disease known as idiopathic intracranial hypertension (IIH), which can be vision-threatening (ICP). It is an uncommon condition with a 0.5–2 per 100 incidence rate [42]. Figure 9b represents an image of IIH.

Hypertensive Retinopathy (HTR): HTN that is not well-controlled impacts the cardiovascular, renal, cerebrovascular, and retinal systems. Target-organ damage is the term for the harm done to these systems. Choroidopathy, retinopathy, and optic neuropathy are the three types of ocular disease caused by HTN that impact the eye. The damage caused by high blood pressure to the retinal arteries is known as hypertensive retinopathy (HTR) shown in Figure 9a. There is strong evidence that the systemic morbidity and mortality caused by TOD are predicted by hypertensive retinopathy. According to a study by Erden et al., the severity and length of HTN are associated with an increase in the incidence of retinopathy [43].

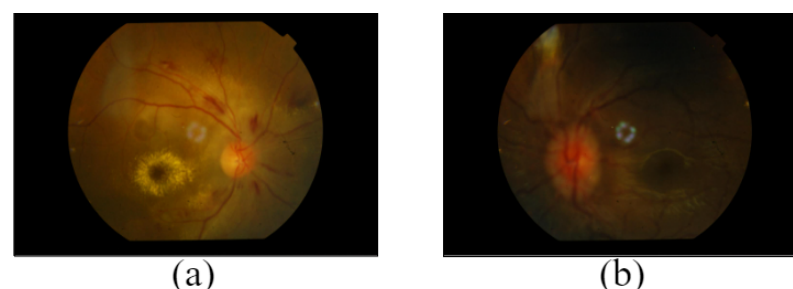


Figure 9. Images of (a) Hypertensive Retinopathy(HTR), (b) Idiopathic Intracranial Hypertension (IIH).

Haemorrhagic Retinopathy (HR): In some retinal diseases, leakage from the retinal blood vessels may cause injury to the retina. This blood flow from retinal blood vessels into the retina leads to hemorrhages shown in Figure 10a. Diabetes, high blood pressure, anemia, and other eye-related diseases, such as macular degeneration, can induce retinal hemorrhages, which can cause temporary or permanent blindness [44]. Hemorrhages exhibit a considerable measure of heterogeneity in shape and appearance [45]. Segmenting hemorrhages in retinal images is challenging since their characteristics resemble some of the dark areas imposed by poor lighting and blood vessels [46].

Laser Scar (LS): For patients who have undergone laser photocoagulation therapy, a specific pathway is created in the diabetic eye-screening programme. The procedure leaves behind circular or atypical scars called laser scars in the retina. Laser scars may appear everywhere in the retinal fundus image except for specific regions such as the optic disc, the macular, and the major vessels shown in Figure 10b [47].

Microaneurysm (MCA): Microaneurysms appear in the retina as small, dispersed red dots as shown in Figure 10c. They are formed due to leakage in blood vessels in the retina. Progressive effects of this disease are lipids and fluids leaking from blood vessels, comprising hard exudates that are yellowish and come in various shapes and sizes [48].

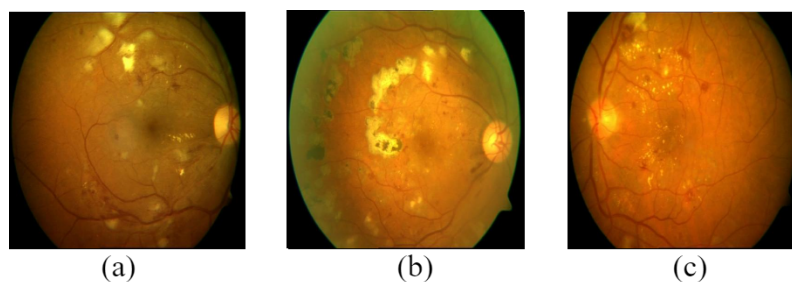


Figure 10. Images of (a) Haemorrhagic Retinopathy (HR), (b) Laser Scar (LS), and (c) Microaneurysm (MCA).

Media Haze (MH): Media Haze is an invisibility in the media known as temporal regions that mainly causes a poor visual analysis of the object or thing being observed. The media opacity caused by media haze is a sign of cataracts, corneal edema, vitreous opacities, or small-sized pupils. The early stage of cataracts is characterized by media haze illness. Media haze identification is necessary for early-stage treatment to lower the risk of cataract-related blindness [49].

Macular Hole (MHL): The foveal center contains a circular, full-thickness opening known as a macular hole (MH). Most of the time, this is unexplained or caused by irregular vitreo-foveal traction [50]. Figure 11a and Figure 11b, respectively, show images of MH and MHL.

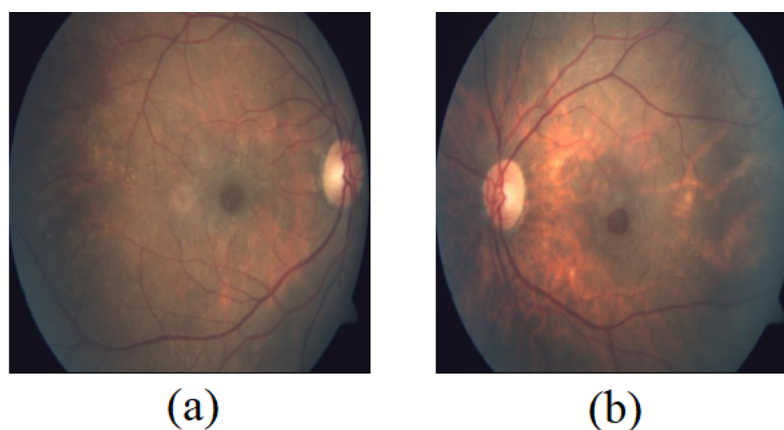


Figure 11. Images of (a) Media Haze (MH), (b) Macular Hole (MHL).

Macular Scar (MS): Macular scars are created after any inflammation, infection, or lesions that were once present have healed. They have an apparent yellow–white center and fluffy borders as shown in Figure 12a [51].

Myopia (MYA): Severe Myopia may lead to irreversible vision loss. Myopia is characterized by pathological abnormalities such as an increase in axial length, fundus tessellation, retina-choroidal degeneration, and an optic disc tilt shown in Figure 12b. Deep learning algorithms are utilized to categorize images of diseases, segment the optic disc, and identify anomalies in fundus images [52]. Myopia can be categorized into two classes. The signs of

low myopia are vision impairment, progressive reduction in vision, ocular discomfort, and whitish or greyish spots in vision. However, the symptoms of high myopia are more severe than those of low myopia, and may result in irreversible disease or complete blindness [53].

Optic Disc Cupping (ODC): Neuroretinal rim in the optic disc appears thinner than the original shape. This condition is usually observed in Glaucoma. High intraocular pressure, which causes Glaucoma, results in the progressive death of the axons and glia that support them [33]. Figure 12c depicts an image of ODC.

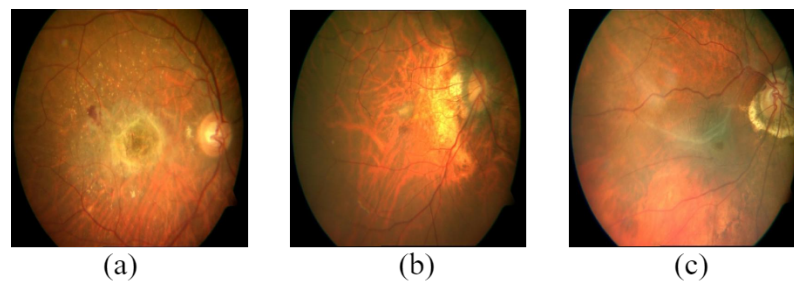


Figure 12. Images of (a) Macular Scar (MS), (b) Myopia (MYA), and (c) Optic Disc Cupping (ODC).

Optic Disc Edema (ODE): The intraocular part of the optic nerve swells due to optic disc edema. The occipital cortex receives the visual signal from retinal ganglion cells, which make up the nerve, via the scleral lamina cribrosa [54].

Optic Disc Pallor (ODP): Observable changes in the neuroretinal rim of the optic disc appear white rather than orange during fundus imaging. ODP indicates that one of several conditions has injured the axons in the optic nerve, which may cause permanent vision loss [33].

Optic Neuritis (ON): Optic neuritis is an inflammatory, demyelinating illness that results in an abrupt, typically single-sided loss of vision. This is closely related to multiple sclerosis (MS). Fifty percent of MS patients experience optic neuritis at some point throughout their illness, presenting as a symptom in 15 to 20 percent of people. Sometimes, various inflammatory and viral disorders affecting the optic nerve are referred to as “optic neuritis” [55]. Images of ODE, ODP, and ON are shown in Figure 13a–c, respectively.

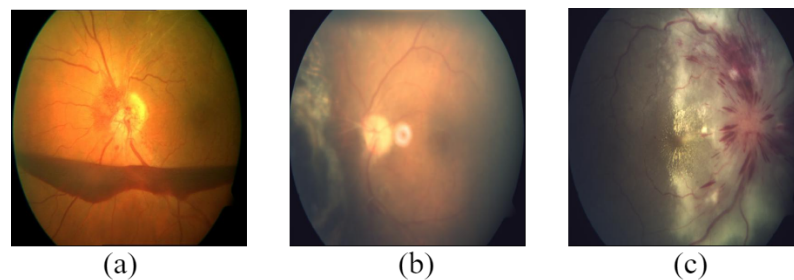


Figure 13. Images of (a) Optic Disc Edema (ODE), (b) Optic Disc Pallor (ODP), and (c) Optic neuritis (ON).

Optic Disc Pit Maculopathy (ODPM): A uncommon unilateral and sporadic congenital malformation of the optic disc is called an optic disc pit. Intraretinal and subretinal fluid at the macula, which results in progressive vision loss, characterize Optic Disc Pit Maculopathy [56]. Figure 14a depicts an image of ODPM.

Preretinal Hemorrhage (PRH): A known side effect of diabetic retinopathy is preretinal bleeding as shown in Figure 13b. Due to blood clots under the internal limiting membrane or in the premacular region between the retina and posterior hyaloid face, patients typically first experience painless loss of vision [57].

Retinal Detachment (RD): When the sensory retina detaches from the retinal pigment epithelium, a condition known as retinal detachment (RD) develops. If this condition is not promptly treated, it can cause severe vision loss [58]. Figure 14c depicts an example of RD.

Retinal Holes and tears (RHL and RTR): Retinal holes and tears are small tears or breaches in the retina as shown in Figure 15a,b. In most cases, holes and tears do not instantly cause severe visual issues. However, retinal tears and holes could become problematic if fluid seeps below the retina. When fluid accumulates behind the retina, it may eventually split from the eye's wall and sustain damage to a portion of the retina. Acute retinal illnesses such as retinal holes and tears can cause complete blindness [59].

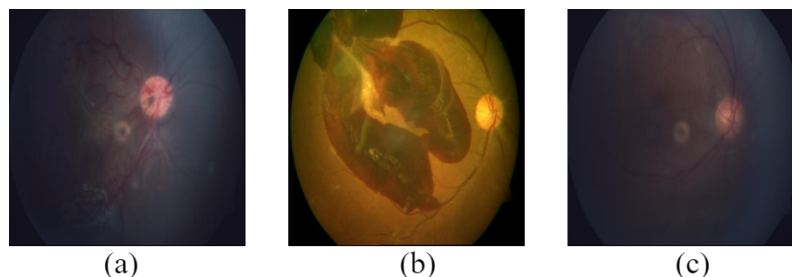


Figure 14. Images of (a) Optic Disc Pit Maculopathy (ODPM), (b) Preretinal Hemorrhage (PRH), and (c) Retinal Detachment (RD).

Retinitis Pigmentosa (RP): Retinitis pigmentosa (RP) is a member of the class of retinal disorders known as pigmentary retinopathies, which includes all retinal dystrophies characterized by a loss of photoreceptors and deposits of pigment in the retina. Pigment deposits predominate in the peripheral retina of people with RP, a retinal degenerative disease, while the central retina is relatively spared. Primary degeneration of the photoreceptor rods and subsequent deterioration of the cones are present in most RP cases. As photoreceptor rods are more impacted than cones in the normal RP, this is often referred to as rod-cone dystrophy. This progression of photoreceptor involvement explains why individuals initially arrive with night blindness and only show visual impairment in daylight situations later in life [60]. Figure 15c depicts an example of RP.

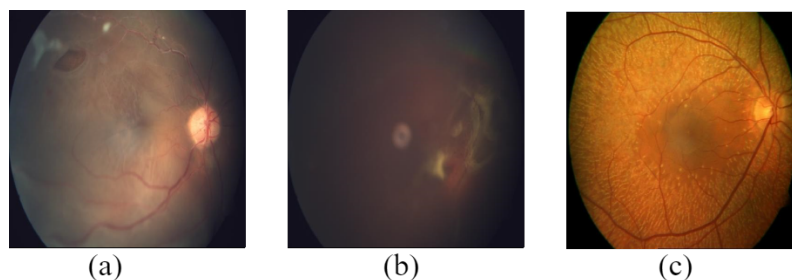


Figure 15. Images of (a,b) Retinal Holes and tears (RHL and RTR), and (c) Retinitis Pigmentosa (RP).

Retinal pigment epithelium changes (RPEC): Age-related reforms in the retinal pigment epithelium (RPE) include the loss of melanin granules, an increase in the density of residual bodies, an accumulation of lipofuscin, an accumulation of basal deposits on or within Bruch's membrane, and the development of drusen [61]. An image of RPEC is shown in Figure 16a.

Retinitis (RS): Retinitis, an inflammation of the retina, can permanently impair vision. A variety of microorganisms can cause retinitis. Various factors, including the patient's age, location, and immunological condition, can influence how these viruses impact them. Retinitis could be the primary eye symptom of significant non-infectious causes such as Behcet illness. Retinitis can manifest as retinochoroiditis or chorioretinitis, depending on the location of initial involvement [62]. Figure 16b shows an example of the RS.

Retinal Traction (RT): RT occurs as a result of traction from membranes in the vitreous or on the retinal surface. It is also known as the separation of the neurosensory retina from the underlying retinal pigment epithelium. Multiple factors have resulted in the formation

of these membranes. However, Diabetes mellitus is the most common cause of RT [56]. Figure 16c shows an example of the RT.

Silicone Oil-Filled Eye (SOFE): In complicated retinal detachments, silicone oil is used increasingly frequently to replace the vitreous shown in Figure 17a. In some otherwise untreatable retinal separations, its use as a tamponade enables effective retinal reattachment [63].

Optociliary Shunt (ST): The vessels that connect the retinal venous system to the choroid on the optic nerve head are called optociliary shunt vessels. Clinical signs include the existence of optociliary shunt veins or peripapillary vascular loops. Vision loss develops gradually as a result of this [56]. Figure 17b shows an example of the ST.

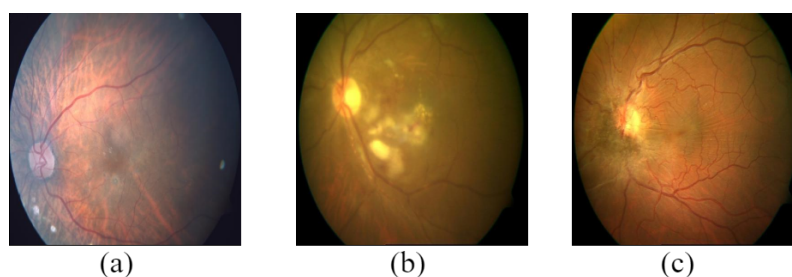


Figure 16. Images of (a) Retinal pigment epithelium changes (RPEC), (b) Retinitis (RS), and (c) Retinal Traction (RT).

Tilted Disc (TD): The optic disc is tilted or obliquely oriented in tilted disc syndrome (TDS), a congenital disc abnormality. Several anomalies of the posterior pole are also linked to this. Using high quality photos, this study analyzes the pathophysiology of TDS and its clinical, functional, and structural effects [64]. An image of TD is shown in Figure 17c.

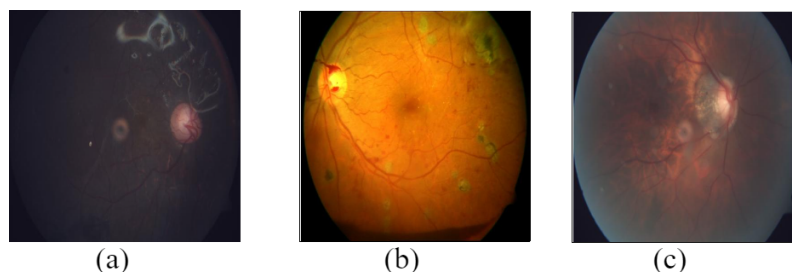


Figure 17. Images of (a) Silicone Oil-Filled Eye (SOFT), (b) Optociliary Shunt (ST), and (c) Tilted Disc (TD).

Tessellation (TSLN): The initial stage of high myopia is referred to as tessellation in the fundus image. The tessellations are visible on the posterior fundus pole as large choroidal vessels (Figure 18a). Grading is assigned to the image, with tessellation depending upon severity [65,66].

Tortuous Vessels (TV): Clinicians recognize vascular tortuosity, or how curled or twisted a blood vessel is, and whether a vein or an artery, appears along its course as a characteristic vascular pattern shown in Figure 18b. Vascular tortuosity is measured by the degree of curve, length of the curled or twisted vessel, and directional changes in vessels. In some studies, the tortuosity is calculated by “vessel arc to chord ratio” or the “vessel curvature” [67].

Vasculitis (VS): Vascular inflammation is known as vasculitis. There are several causes, but only a few histologic forms, of vascular inflammation results. Any vessel in any organ might be impacted, leading to a wide range of indications and symptoms. The diagnosis of particular types of vasculitis is made more difficult by these unpredictable clinical symptoms and the etiologic nonspecificity of the histologic abnormalities. This is a concern because various vasculitides have drastically varying prognoses and therapies

despite having similar clinical presentations—small vessel vasculitis is depicted in the Figure 18c [68].

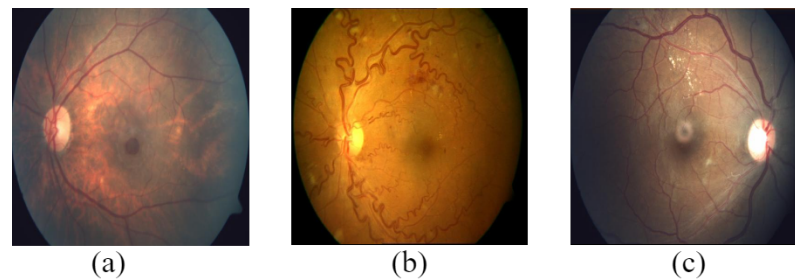


Figure 18. Images of (a) Tesselation (TSLN), (b) Tortuous Vessels (TV), and (c) Vasculitis (VS).

The ophthalmologists examine and label each fundus image. However, several diseases may be associated with a single image. Therefore, the newly created dataset is a multi-label imbalanced dataset. The Table 2 provides a summary of the number of labels assigned to each image.

Table 2. Summary of the assignment of labels to number of fundus images in a multilabelled database.

Sr. No.	Normal/Disease	Fundus Images	Sr. No.	Normal/Disease	Fundus Images
1	WNL	262	26	MH	41
2	AH	2	27	MHL	7
3	AION	4	28	MS	31
4	ARMD	10	29	MYA	43
5	BRVO	22	30	ODC	37
6	CB	4	31	ODE	20
7	CF	7	32	ODP	18
8	CL	6	33	ON	2
9	CNV	2	34	OPDM	1
10	CRAO	1	35	PRH	12
11	CRS	41	36	RD	16
12	CRVO	12	37	RHL	1
13	CSR	16	38	RTR	2
14	CWS	31	39	RP	4
15	CSC	1	40	RPEC	4
16	DN	6	41	RS	8
17	DR	70	42	RT	41
18	EDN	70	43	SOFE	4
19	ERM	5	44	ST	4
20	GRT	1	45	TD	16
21	HPED	3	46	TSLN	37
22	HR	86	47	TV	18
23	LS	16	48	VS	7
24	MCA	8	49	HTN	11
25	ME	41	50	IIH	6

4. Conclusions

We collected data from a reputable ophthalmic research facility center. Medical specialists analyze the retinal fundus images to diagnose eye conditions and accurately recommend the most appropriate treatment. We noticed that the data included widely identified diseases. However, when gathering data, rare diseases are also recognized, which leads to an imbalance in the data. Additionally, many retinal fundus images have two or more diseases or findings. Retinal Fundus Multi-Disease Dataset 2.0 is the second Multilabel Imbalanced Dataset containing more than 45 diseases, as far as is known. The classifications

in this database are challenging to the research society. The development of computer systems allowing for AI-based illness diagnostics might help ophthalmologists.

Author Contributions: Conceptualization, M.K., S.P. (Sachin Panchal), S.P. (Samiksha Pachade) and A.N.; Methodology, S.P. (Sachin Panchal), R.N., P.P. and A.B.; Resources, R.N. and P.P.; Validation, P.P. and A.B.; Formal analysis and investigation, M.K. and R.N.; Data curation, S.P. (Sachin Panchal) and A.N.; Writing—original draft preparation, S.P. (Sachin Panchal); Writing—review and editing, M.K., S.P. (Samiksha Pachade), P.P., A.B. and R.N.; Visualization, S.P. (Sachin Panchal), S.P. (Samiksha Pachade) and A.N.; Supervision, M.K.; Project administration, M.K. All authors have read and agreed to the published version of the manuscript.

Funding: This research received no external funding.

Institutional Review Board Statement: The study was conducted according to the ethics of clinical practices and medical research and approved by the Institutional Review Board of Shri Guru Gobind Singhji Institute of Engineering and Technology, Nanded, India.

Informed Consent Statement: Informed consent was obtained from all subjects involved in the study.

Data Availability Statement: This dataset is available for download at: <https://zenodo.org/record/7505822>.

Acknowledgments: The authors are very grateful to our institute and the Technical Education Quality Improvement Program (TEQIP). TEQIP, the World Bank project provided a state-of-the-art Center of Excellence research lab in Signal and Image Processing. We thank Amit Rathod (Yashwantrao Chavan Memorial Hospital, Pune, MH, India) and Ganesh Naidu (Ganapati Netralaya, Jalna, MH, India) for their assistance in data collection.

Conflicts of Interest: The authors declare no conflict of interest.

References

1. Vision Impairment and Blindness. Available online: <https://www.who.int/news-room/fact-sheets/detail/blindness-and-visual-impairment> (accessed on 13 October 2022).
2. Jelinek, H.; Cree, M.J. *Automated Image Detection of Retinal Pathology*; CRC Press: Boca Raton, FL, USA, 2009.
3. Cen, L.P.; Ji, J.; Lin, J.W.; Ju, S.T.; Lin, H.J.; Li, T.P.; Wang, Y.; Yang, J.F.; Liu, Y.F.; Tan, S.; et al. Automatic detection of 39 fundus diseases and conditions in retinal photographs using Deep Neural Networks. *Nat. Commun.* **2021**, *12*. [[CrossRef](#)] [[PubMed](#)]
4. Brown, G.C.; Brown, M.M.; Hiller, T.; Fischer, D.; Benson, W.E.; Magargal, L.E. Cotton-wool spots. *Retina* **1985**, *5*, 206–214. [[CrossRef](#)] [[PubMed](#)]
5. Shabbir, A.; Rasheed, A.; Shehraz, H.; Saleem, A.; Zafar, B.; Sajid, M.; Ali, N.; Dar, S.H.; Shehryar, T. Detection of glaucoma using retinal fundus images: A comprehensive review. *Math. Biosci. Eng.* **2021**, *18*, 2033–2076. [[CrossRef](#)] [[PubMed](#)]
6. Mary, V.S.; Rajsingh, E.B.; Naik, G.R. Retinal fundus image analysis for diagnosis of glaucoma: A comprehensive survey. *IEEE Access* **2016**, *4*, pp. 4327–4354. [[CrossRef](#)]
7. Catania, C.A.; Bromberg, F.; Garino, C.G. An autonomous labeling approach to support vector machines algorithms for network traffic anomaly detection. *Expert Syst. Appl.* **2012**, *39*, 1822–1829. [[CrossRef](#)]
8. Huang, Y.M.; Hung, C.M.; Jiau, H.C. Evaluation of neural networks and data mining methods on a credit assessment task for class imbalance problem. *Nonlinear Anal. Real World Appl.* **2006**, *7*, 720–747. [[CrossRef](#)]
9. Jain, A.; Ratnoo, S.; Kumar, D. Addressing class imbalance problem in medical diagnosis: A genetic algorithm approach. In Proceedings of the 2017 International Conference on Information, Communication, Instrumentation and Control (ICICIC), Indore, India, 17–19 August 2017; pp. 1–8. [[CrossRef](#)]
10. Tarekegn, A.; Ricceri, F.; Costa, G.; Ferracin, E.; Giacobini, M. Predictive modeling for frailty conditions in elderly people: Machine learning approaches. *JMIR Med. Inform.* **2020**, *8*, e16678. [[CrossRef](#)]
11. Bullock, J.; Luccioni, A.; Pham, K.H.; Lam, C.S.N.; Luengo-Oroz, M. Mapping the landscape of artificial intelligence applications against COVID-19. *J. Artif. Intell. Res.* **2020**, *69*, 807–845. [[CrossRef](#)]
12. Topcon TRC NW300—Topcon Europe Medical—PDF Catalogs | Technical Documentation. Available online: <https://pdf.medicalexpo.com/pdf/topcon-europe-medical/topcon-trc-nw300/77876-75596.html> (accessed on 23 October 2022).
13. Zeiss FF450plus Fundus Camera with VISUPAC | Technical Brochure. Available online: <https://www.zeiss.com/content/dam/Meditec/us/brochures/ff450plus-visupac-cap-en-us-31-020-0025i.pdf> (accessed on 23 October 2022).
14. Paulus, J.; Meier, J.; Bock, R.; Hornegger, J.; Michelson, G. Automated quality assessment of retinal fundus photos. *Int. J. Comput. Assist. Radiol. Surg.* **2010**, *5*, 557–564. [[CrossRef](#)]
15. Sun, Y.; Smith, L.E. Retinal vasculature in development and diseases. *Annu. Rev. Vis. Sci.* **2018**, *4*, 101. [annurev-vision-091517-034018](https://doi.org/10.1146/annurev-vision-091517-034018). [[CrossRef](#)]

16. Tripathy, K. Asteroid hyalosis. *N. Engl. J. Med.* **2018**, *379*, e12. [[CrossRef](#)]
17. Fontal, M.R.; Kerrison, J.B.; Garcia, R.; Oria, V. Ischemic optic neuropathy. *Semin. Neurol.* **2007**, *27*, 221–232. [[CrossRef](#)]
18. Hayreh, S.S. Ischemic optic neuropathy. *Prog. Retin. Eye Res.* **2009**, *28*, 34–62. [[CrossRef](#)]
19. Nowak, J.Z. Age-related macular degeneration (AMD): Pathogenesis and therapy. *Pharmacol. Rep.* **2006**, *58*, 353.
20. DeAngelis, M.M.; Owen, L.A.; Morrison, M.A.; Morgan, D.J.; Li, M.; Shakoor, A.; Vitale, A.; Iyengar, S.; Stambolian, D.; Kim, I.K.; et al. Genetics of age-related macular degeneration (AMD). *Hum. Mol. Genet.* **2017**, *26*, R45–R50. ddx228. [[CrossRef](#)]
21. Kösea, C.; Sevika, U.; Gençalioglu, O. Automatic segmentation of age-related macular degeneration in retinal fundus images. *Comput. Biol. Med.* **2008**, *38*, 611–619. [[CrossRef](#)]
22. Jager, R.D.; Mieler, W.F.; Miller, J.W. Age-Related Macular Degeneration. *N. Engl. J. Med.* **2008**, *358*, 2606–2617. [[CrossRef](#)]
23. Rogers, S.; McIntosh, R.; Cheung, N.; Lim, L.; Wang, J.; Mitchell, P.; Kowalski, J.; Nguyen, H.; Wong, T. International Eye Disease Consortium: The prevalence of retinal vein occlusion: Pooled data from population studies from the United States, Europe, Asia, and Australia. *Ophthalmology* **2010**, *117*, 313–319. [[CrossRef](#)]
24. Gopal, L.; Badrinath, S.S.; Kumar, K.; Doshi, G.; Biswas, N. Optic Disc in Fundus Coloboma. *Ophthalmology* **1996**, *103*, 2120–2127. [[CrossRef](#)]
25. Grosso, D.; Borrelli, E.; Sacconi, R.; Bandello, F.; Querques, G. Recognition, diagnosis and treatment of chorioretinal folds: Current perspectives. *Clin. Ophthalmol.* **2020**, *14*, 3403. [[CrossRef](#)]
26. Henkind, P.; Wise, G.N. Retinal neovascularization, collaterals, and vascular shunts. *Br. J. Ophthalmol.* **1974**, *58*, 413. [[CrossRef](#)] [[PubMed](#)]
27. Rotsos, T.G.; Moschos, M.M. Cystoid macular edema. *Clin. Ophthalmol.* **2008**, *2*, 919–930. [[CrossRef](#)] [[PubMed](#)]
28. Tang, M.C.S.; Teoh, S.S.; Ibrahim, H.; Embong, Z. Neovascularization detection and localization in fundus images using deep learning. *Sensors* **2021**, *21*, 5327. [[CrossRef](#)] [[PubMed](#)]
29. Hayreh, S. Central retinal artery occlusion. *Indian J. Ophthalmol.* **2018**, *66*, 1684_1446_18. [[CrossRef](#)]
30. Chorioretinitis—Statpearls—NCBI Bookshelf. Available online: <https://www.ncbi.nlm.nih.gov/books/NBK551705/> (accessed on 28 October 2022).
31. Cheung, N.; Klein, R.; Wang, J.J.; Cotch, M.F.; Islam, A.F.; Klein, B.E.; Cushman, M.; Wong, T.Y. Traditional and novel cardiovascular risk factors for retinal vein occlusion: The multiethnic study of atherosclerosis. *Investig. Ophthalmol. Vis. Sci.* **2008**, *49*, 4297–4302. [[CrossRef](#)]
32. Rebika, D.; Saranya, D.; Kavitha, D.; Parijat, C.; Murugesan, V.; Radhika, T.; Sen, S. Cysticercosis of the eye. *Int. J. Ophthalmol.* **2017**, *10*, 1319–1324. [[CrossRef](#)]
33. Optic Disc Pallor: Ophthalmoscopic Abnormalities: The Eyes Have It. Available online: http://kellogg.umich.edu/theeyeshaveit/opticfundus/disc_pallor.html (accessed on 28 October 2022).
34. Schmidt, D. The mystery of cotton-wool spots—a review of recent and historical descriptions. *Eur. J. Med. Res.* **2008**, *13*, 231.
35. Mittal, D.; Kumari, K. Automated detection and segmentation of drusen in retinal fundus images. *Comput. Electr. Eng.* **2015**, *47*, 82–95. [[CrossRef](#)]
36. Wang, W.; Lo, A.C. Diabetic retinopathy: Pathophysiology and treatments. *Int. J. Mol. Sci.* **2018**, *19*, 1816. ijms19061816. [[CrossRef](#)]
37. Kempen, J.H.; O’Colmain, B.J.; Leske, M.C.; Haffner, S.M.; Klein, R.; Moss, S.E.; Taylor, H.R.; Hamman, R.F.; The prevalence of diabetic retinopathy among adults in the United States. *Arch. Ophthalmol.* **2004**, *122*, 552–563. [[CrossRef](#)]
38. Panchal, S.; Kokare, M. A Comprehensive Survey on the Detection of Diabetic Retinopathy. *IETE J. Res.* **2022**. [[CrossRef](#)]
39. American Society of Retina Specialists, Epiretinal Membranes. Available online: <https://www.asrs.org/patients/retinal-diseases/19/epiretinal-membranes> (accessed on 22 November 2022).
40. Berrocal, M.; Chenworth, M.; Acaba, L. Management of giant retinal tear detachments. *J. Ophthalmic Vis. Res.* **2017**, *12*, 93. [[CrossRef](#)]
41. Kim, L.A.; Lee, S.Y.; Thorell, M.R.; Tripathy, K.; Barros, N.; Hacopian, A.; Kiernan, D.F.; Bhagat, N.; Lim, J.I.; Jung, E.E. Pigment Epithelial Detachment. Available online: https://eyewiki.aao.org/Pigment_Epithelial_Detachment (accessed on 22 November 2022).
42. Sargues, L.R.; Sanchis, M.I.S.; Adsuara, C.M.; Villanueva, C.G.; Salvador, B.L.; Taulet, E.C. Incidental idiopathic intracranial hypertension. *Rom. J. Ophthalmol.* **2021**, *65*, 187. [[CrossRef](#)]
43. Modi, P.; Arsiwalla, T. Hypertensive retinopathy. In *StatPearls [Internet]*; StatPearls Publishing: St. Petersburg, FL, USA, 2022.
44. Kaur, N.; Chatterjee, S.; Acharyya, M.; Kaur, J.; Kapoor, N.; Gupta, S. A supervised approach for automated detection of hemorrhages in retinal fundus images. In Proceedings of the 2016 5th International Conference on Wireless Networks and Embedded Systems (WECON), Rajpura, India, 14–16 October 2016; pp. 1–5. [[CrossRef](#)]
45. Tang, L.; Niemeijer, M.; Reinhardt, J.M.; Garvin, M.K.; Abramoff, M.D. Splat feature classification with application to retinal hemorrhage detection in fundus images. *IEEE Trans. Med. Imaging* **2012**, *32*, 364–375. [[CrossRef](#)]
46. Aziz, T.; Ilesanmi, A.E.; Charoenlarnopparut, C. Efficient and Accurate Hemorrhages Detection in Retinal Fundus Images Using Smart Window Features. *Appl. Sci.* **2021**, *11*, 6391. [[CrossRef](#)]
47. Wei, Q.; Li, X.; Wang, H.; Ding, D.; Yu, W.; Chen, Y. Laser scar detection in fundus images using convolutional neural networks. In *Computer Vision—ACCV 2018*; Springer: Cham, Switzerland, 2018; pp. 191–206.12. [[CrossRef](#)]

48. Benzamin, A.; Chakraborty, C. Detection of hard exudates in retinal fundus images using deep learning. In Proceedings of the 2018 Joint 7th International Conference on Informatics, Electronics & Vision (ICIEV) and 2018 2nd International Conference on Imaging, Vision & Pattern Recognition (icIVPR), Kitakyushu, Japan, 25–29 June 2018; pp. 465–469. [[CrossRef](#)]
49. Sengar, N.; Joshi, R.C.; Dutta, M.K. An Efficient Artificial Intelligence-based approach for Diagnosis of Media Haze Disease. In Proceedings of the 2021 12th International Conference on Computing Communication and Networking Technologies (ICCCNT), Kharagpur, India, 6–8 July 2021; pp. 1–6. [[CrossRef](#)]
50. Kim, K.M.; Heo, T.Y.; Kim, A.; Kim, J.; Han, K.J.; Yun, J.; Min, J.K. Development of a fundus image-based deep learning diagnostic tool for various retinal diseases. *J. Pers. Med.* **2021**, *11*, 321. [[CrossRef](#)]
51. Bahia-Oliveira, L.M.; Rangel, A.L.; Boechat, M.S.; Mangiavacchi, B.M.; Martins, L.M.; Ferraz, F.B.; Almeida, M.B.; Peixoto, E.M.W.; Vieira, F.P.; Peixe, R.G. Immunological and immunogenetic parameters on the diversity of ocular toxoplasmosis: Evidence to support morphological criteria to classify retinal/retinochoroidal scar lesions in epidemiologic surveys. In *Toxoplasmosis-Recent Advances*; IntechOpen: London, UK, 2012. [[CrossRef](#)]
52. Devda, J.; Eswari, R. Pathological myopia image analysis using deep learning. *Procedia Comput. Sci.* **2019**, *165*, 239–244. [[CrossRef](#)]
53. Wan, C.; Li, H.; Cao, G.F.; Jiang, Q.; Yang, W.H. An Artificial Intelligent Risk Classification Method of High Myopia Based on Fundus Images. *J. Clin. Med.* **2021**, *10*, 4488. [[CrossRef](#)]
54. Urfalioglu, S.; Ozdemir, G.; Guler, M.; Duman, G.G. The evaluation of patients with optic disc edema: A retrospective study. *North. Clin. Istanb.* **2021**, *8*, 280. [[CrossRef](#)]
55. Benjamin, O. Optic Neuritis: Pathophysiology, Clinical Features, and Diagnosis. Available online: <https://www.uptodate.com/contents/optic-neuritis-pathophysiology-clinical-features-and-diagnosis> (accessed on 12 December 2022).
56. Pachade, S.; Porwal, P.; Thulkar, D.; Kokare, M.; Deshmukh, G.; Sahasrabuddhe, V.; Giancardo, L.; Quéllec, G.; Mériaudeau, F. Retinal fundus multi-disease image dataset (RFMiD): A dataset for multi-disease detection research. *Data* **2021**, *6*, 14. [[CrossRef](#)]
57. Karagiannis, D.; Kontadakis, G.A.; Flanagan, D. ND: YAG laser for preretinal hemorrhage in diabetic retinopathy. *Am. J. Ophthalmol. Case Rep.* **2018**, *10*, 8–9. [[CrossRef](#)] [[PubMed](#)]
58. Li, Z.; Guo, C.; Nie, D.; Lin, D.; Zhu, Y.; Chen, C.; Wu, X.; Xu, F.; Jin, C.; Zhang, X.; et al. Deep learning for detecting retinal detachment and discerning macular status using ultra-widefield fundus images. *Commun. Biol.* **2020**, *3*, 15. [[CrossRef](#)] [[PubMed](#)]
59. Russel, L. Retinal Holes and Tears. Available online: <https://www.optometrists.org/general-practice-optometry/guide-to-eye-conditions/guide-to-retinal-diseases/retinal-holes-and-tears/> (accessed on 23 December 2022).
60. Hamel, C. Retinitis pigmentosa. *Orphanet J. Rare Dis.* **2006**, *1*, 1–12. [[CrossRef](#)] [[PubMed](#)]
61. Bonilha, V.L. Age and disease-related structural changes in the retinal pigment epithelium. *Clin. Ophthalmol.* **2008**, *2*, 413–424. [[CrossRef](#)]
62. Gupta, K.; Tripathy, N. Retinitis. Available online: <https://pubmed.ncbi.nlm.nih.gov/32809355/> (accessed on 22 December 2022).
63. Gonvers, M. Temporary Silicone Oil Tamponade in the Management of Retinal Detachment with Proliferative Vitreoretinopathy. *Am. J. Ophthalmol.* **1985**, *100*, 239–245. [[CrossRef](#)]
64. Cohen, S.Y.; Vignal-Clermont, C.; Trinh, L.; Ohno-Matsui, K. Tilted disc syndrome (TDS): New hypotheses for posterior segment complications and their implications in other retinal diseases. *Prog. Retin. Eye Res.* **2021**, *88*, 101020. [[CrossRef](#)]
65. Ohno-Matsui, K.; Lai, T.Y.; Lai, C.C.; Cheung, C.M.G. Updates of pathologic myopia. *Prog. Retin. Eye Res.* **2016**, *52*, 156–187. [[CrossRef](#)]
66. Lyu, H.; Chen, Q.; Hu, G.; Shi, Y.; Ye, L.; Yin, Y.; Fan, Y.; Zou, H.; He, J.; Zhu, J.; et al. Characteristics of Fundal Changes in Fundus Tessellation in Young Adults. *Front. Med.* **2021**, *8*, 616249. [[CrossRef](#)]
67. Joshi, V.; Reinhardt, J.M.; Abramoff, M.D. Automated measurement of retinal blood vessel tortuosity. In *Medical Imaging 2010: Computer-Aided Diagnosis, Proceedings of the SPIE Medical Imaging, San Diego, CA, USA, 13–18 February 2010*; SPIE: Bellingham, WA, USA, 2010; Volume 7624, pp. 929–937. [[CrossRef](#)]
68. Jennette, J.C.; Falk, R.J. Small-Vessel Vasculitis. *N. Engl. J. Med.* **1997**, *337*, 1512–1523. [[CrossRef](#)]

Disclaimer/Publisher’s Note: The statements, opinions and data contained in all publications are solely those of the individual author(s) and contributor(s) and not of MDPI and/or the editor(s). MDPI and/or the editor(s) disclaim responsibility for any injury to people or property resulting from any ideas, methods, instructions or products referred to in the content.